Energy Conversion and Management 258 (2022) 115537

Contents lists available at ScienceDirect

Energy Conversion and Management

journal homepage: www.elsevier.com/locate/enconman

Optimization of agricultural resources in water-energy-food nexus in complex environment: A perspective on multienergy coordination

Mo Li [a,b], Li Zhao [a], Chenglong Zhang [c], Yangdachuan Liu [d], Qiang Fu [a,b,*]

[a] School of Water Conservancy & Civil Engineering, Northeast Agricultural University, Harbin, Heilongjiang 150030, China
[b] Key Laboratory of Effective Utilization of Agricultural Water Resources of Ministry of Agriculture, Northeast Agricultural University, Harbin, Heilongjiang 150030, China
[c] Center for Agricultural Water Research in China, China Agricultural University, Beijing 100083, China
[d] Heilongjiang Agricultural Engineering Vocational College, Harbin, Heilongjiang 150030, China

ARTICLE INFO

Keywords:
Water-energy-food nexus
Irrigated agriculture
Optimization modeling
Multiobjective
Multienergy synergy
Left–right type fuzzy numbers

ABSTRACT

Synergistic regulation of various agricultural resources in agricultural water-energy-food nexus systems is important for understanding the key regulatory processes and related synergistic relationships. However, regulation with the goal of multienergy interaction and coordination to adapt to environmental changes is extremely challenging. As a solution to the problem, an uncertainty-based modeling approach is proposed for the optimal regulation of water, soil and energy resources from a multienergy synergy perspective by integrating multiobjective nonlinear programming, left–right type fuzzy numbers and credibility programming into a framework. The approach aims to assess the interactions and synergistic relationships among biomass electrical energy, light energy, and hydroelectric energy, clarify the dynamic characteristics of resource allocation and socioeconomic and environmental effects, and capture the high uncertainty in the nexus area. This study contributes to the efficient and sustainable management of agricultural water, energy and land resources. The approach was tested and implemented based on a case study of Jinxi Irrigation District in China. The results reveal that there are trade-offs and games among the light use efficiency, hydroelectric energy and biomass energy, and their coordination enhances the system synergy among resources, the economy and the environment by 12.22%, with a 2.67% increase in the irrigation water use efficiency and a 4.92% increase in the energy use efficiency. Uncertainties significantly affect the synergy among multiple energies. More water will promote collaborative energy management, with the coordination development degree will increase by 2.20% when the water quantity increases by 4.16%, however, it accompanied higher water scarcity risks.

1. Introduction

Water, food, and energy are essential and closely related life support requirements for human well-being and sustainable development, and these requirements are closely interconnected [1]. For example, water is used to produce food and energy; energy is required to pump and distribute water and to manufacture, harvest, store, and transport food; and crop and food waste materials can be employed for energy production [2]. Continued global population growth places high demands on the water, energy and food (WEF) resources needed to maintain a healthy standard of living [3]. Agricultural production is the largest global water user, accounting for approximately 90% of global freshwater consumption over the past century. Approximately 30% of global energy consumption originates from food production and supply [4]. Agricultural irrigation provides approximately 40% of the world's food, and therefore, agricultural nexus management should be studied.

There are currently many studies of agricultural nexus management [5]. Optimization models are very effective nexus management methods to quantify interactions and determine the optimal allocation of resources, such as agricultural land and water resources [6]. For example, Ma et al. [7] studied the synergistic management of water-food-ecology-energy systems and developed a bilevel decentralized chance-constrained programming water-food-ecology-energy model to obtain optimal management solutions regarding water allocation, food production, and power generation. Zuo et al. [8] investigated agricultural WEF and area management and developed a scenario-based type-2 fuzzy

* Corresponding author at: School of Water Conservancy & Civil Engineering, Northeast Agricultural University, Harbin, Heilongjiang 150030, China.
E-mail address: fuqiang0629@126.com (Q. Fu).

https://doi.org/10.1016/j.enconman.2022.115537
Received 21 December 2021; Received in revised form 10 March 2022; Accepted 22 March 2022
Available online 28 March 2022

interval programming-water-energy-food nexus (WEFN) model for agricultural net profit maximization to achieve synergistic resource allocation in a coupled WEF system. Zhang et al. [9] developed a socioeconomic model based on the WEFN framework to quantitatively analyze multidimensional indicators and assist decision makers in achieving economic efficiency. In contrast, most contemporary studies have been conducted by optimizing agricultural resources with the main objective of maximizing food production or the net profits originating from agriculture [10]. However, it is not sustainable to consider only food production or maximizing the net profitability of agriculture as the main goal. In the context of resource/energy scarcity, resource/energy use efficiency has received equal attention to save resources and promote efficient agriculture. However, the existing studies on managing agricultural WEFN systems based on optimization modeling have generally not quantified or provided decision support for energy-related factors; notably, most researchers have established the relationships among elements in a WEFN for one energy type, such as electricity [11] or bioenergy [12].

In fact, energy is crucial in nexus systems and exists in many forms. The crop yield formation process and other growth stages require water uptake in the presence of solar radiation, which affects stomatal conductance and, consequently, light use efficiency [13]. Increasing the light use efficiency facilitates enhanced biomass accumulation in crops, which in turn increases food production. As such, food production depends on the light use efficiency [14]. In addition to light, crops also require electrical energy for water lifting, transport, irrigation and drainage in the crop formation process. Moreover, crops produce biowaste such as straw in the yield formation process, thus providing the raw material for biomass energy production; notably, some biomass energy can be converted into biomass electrical energy through vaporization and combustion [15]. In agriculture WEFN systems, these forms of energy interact with each other, and there are trade-offs and games, and they are influenced by the utilization of agricultural resources, such as water, soil, and energy resources. In turn, the synergy among these three energy sources further affects the integrated allocation of agricultural resources and thus impacts food production. However, due to the ease of quantification, most of the existing agricultural WEFN optimization model studies focused on quantifying the utilization of electrical energy during the crop growth cycle. Since light use efficiency is associated with the dynamic process of the crop water cycle, which is complex to quantify and optimize in a modelling framework, existing models of agricultural WEFN rarely consider the light use efficiency during crop growth. In addition, some scholars have quantified the production potential of crop waste-based biomass energy during the crop life cycle in their modeling, often ignoring the ability of bioenergy to then further produce bioelectricity. Because bioelectricity is recyclable in agricultural systems, quantifying this energy fraction is essential. Therefore, optimization models that account for agricultural WEFN systems and consider optimal agricultural water, soil, and energy resource regulation based on the synergy among light energy, biomass electrical energy, and electrical energy, are necessary and challenging to develop.

In the process of water, soil and energy resource optimization in a coupled WEFN system, the transformation processes in the atmospheric water-surface water-soil water-groundwater cycle are involved. Specifically, surface water, soil water and groundwater are returned to the atmosphere through evaporation and become an important component of atmospheric water. Moreover, there is a constant exchange of water among surface water, soil water and groundwater and among areas in various regions [16]. These interactions influence the dynamic nature of water allocation in different growth stages, and considering them can lead to more accurate multiwater allocation schemes by dynamically reflecting the relationships among irrigation, precipitation, water consumption, and water demand in irrigation areas.

In addition, from the perspective of data acquisition, the multienergy coordination models of agricultural WEFN involve large numbers of parameters that are obtained and processed from uncertain raw data. Varying observation and measurement accuracies, changing socioeconomic and natural conditions, and data integration uncertainty are attributed to fluctuations in model inputs. In particular, the quantification and synergy of multiple energy sources in an agricultural WEFN are closely related to the water cycle, and the relevant parameters dynamically change. To quantitatively reflect and address the uncertainty in the multienergy regulation of agricultural WEFN systems, uncertainty programming can be coupled with a nexus model. The classic uncertainty programming methods include stochastic mathematical programming (SMP), fuzzy mathematical programming (FMP) and interval mathematical programming (IMP). Each of these methods has distinct advantages and limitations. SMP can effectively handle a wide range of probabilistic uncertainties in decision making. However, the high computational data requirements for specifying parameter probability distributions may affect the practical application of SMP methods. IMP has lower data requirements for handling uncertain parameters but may encounter difficulties when highly uncertain parameters are present on the right-hand side of model constraint equations. FMP can provide a good balance between data requirements and information accuracy. Multienergy coordination in an agricultural WEFN involves many parameters that are associated with weather, hydrology, agronomy, the economy and the environment. Thus, FMP is most appropriate for use in models in terms of the accurate expression of uncertainty and high computational efficiency. Most of the existing FMP literature has focused on triangular fuzzy numbers due to their simple form. LR-type fuzzy numbers are more common fuzzy numbers, and many types of fuzzy numbers, such as triangular, trapezoidal, and exponential, can be expressed with this formulation. LR-type fuzzy numbers have a broad application scope and can be used to quantify various uncertain parameters with different characteristics [17]. In addition, as a widely used fuzzy programming method, credibility programming, with the characteristic of self-duality, which can replace likelihood and necessity [18], is able to effectively address constraint-violation issues in multienergy coordination models because available water and energy are usually changing. Therefore, the integration of LR-type fuzzy numbers and the credibility constraint method is a potential approach to effectively manage the uncertainty in multi-energy synergy in the agricultural WEFN.

Based on the above information, an optimal model of agricultural water and soil resource allocation is developed under complex fuzzy uncertainty from a multienergy synergy perspective (LR-FN-MONLP). This model combines LR-type fuzzy numbers and plausibility constraints into a multiobjective nonlinear programming method to achieve soil and water energy resource allocation for a WEFN based on the synergy among three energy sources (light energy, biomass electrical energy, and hydroelectric energy). This study explores the interactions and synergistic relations among biomass electrical energy, light energy, and hydroelectric energy in agricultural systems, and the results can efficiently and sustainably aid in the management of agricultural, water, energy and land resources from the perspective of multienergy coordination considering environmental changes. This study includes the following steps: (1) The complex fuzzy uncertainties associated with the parameters and constraints in the LR-FN-MONLP model are quantified with LR-type fuzzy numbers and plausibility constraints. (2) A multiobjective nonlinear programming model with coupled water cycle equations and synergistic functions for light use efficiency, biomass electrical energy and hydroelectric energy utilization is established for the cooperative regulation and optimization of water, soil and energy resources. (3) The model is solved with possibilistic mean value-based, credibility constraint and normalization methods to analyze the dynamic use of soil and water energy resources, the synergy among the above three energy sources and the corresponding socioeconomic-environmental effects. The model is subsequently applied in the Jinxi Irrigation District, Northeast China.

2. Method

The framework of the LR-FN-MONLP model constructed in this paper includes a multiobjective nonlinear optimization model that incorporates LR-type fuzzy numbers and plausibility constraints. Specifically, the model integrates LR-type fuzzy numbers and plausibility constraints into the main framework of multiobjective nonlinear programming.

2.1. Multiobjective nonlinear programming

The main framework of the LR-FN-MONLP model constructed in this paper is multiobjective nonlinear programming [19], which is used to address multiobjectivity and nonlinearity issues in optimization problems and can be expressed as follows:

$$Z = F(x_1, x_2, \cdots, x_n) = \begin{pmatrix} max(min) f_1(x_1, x_2, \cdots, x_n) \\ max(min) f_2(x_1, x_2, \cdots, x_n) \\ \vdots \\ max(min) f_k(x_1, x_2, \cdots, x_n) \end{pmatrix} \tag{1}$$

subject to.

$$H(x_1, x_2, \cdots, x_n) = \begin{pmatrix} h_1(x_1, x_2, \cdots, x_n) \\ h_2(x_1, x_2, \cdots, x_n) \\ \vdots \\ h_m(x_1, x_2, \cdots, x_n) \end{pmatrix} = 0 \tag{2}$$

$$G(x_1, x_2, \cdots, x_n) = \begin{pmatrix} g_1(x_1, x_2, \cdots, x_n) \\ g_2(x_1, x_2, \cdots, x_n) \\ \vdots \\ g_l(x_1, x_2, \cdots, x_n) \end{pmatrix} \geqslant 0 \tag{3}$$

$$x_1, x_2, \cdots, x_n \geqslant 0 \tag{4}$$

where $[x_1, x_2, \cdots, x_n]^T$ is the vector of decision variables. $Z = F(x_1, x_2, \cdots, x_n)$ is a k-dimensional function vector, and k is the number of scalar objective functions. $H(x_1, x_2, \cdots, x_n)$ is an m-dimensional function vector, and m is the number of scalar constraints. $G(x_1, x_2, \cdots, x_n)$ is an n-dimensional function vector, and n is the number of scalar constraints At least one of the functions$F(x_1, x_2, \cdots, x_n)$,$H(x_1, x_2, \cdots, x_n)$, or $G(x_1, x_2, \cdots, x_n)$ is a non-linear function of the decision vector$[x_1, x_2, \cdots, x_n]^T$.

2.2. Left-right type fuzzy numbers

LR-type fuzzy numbers can resolve the problem of fuzzy variable quantification in optimization problems, and LR-type fuzzy numbers can be described with the following affiliation functions:

$$A(u) = \begin{cases} L\left(\frac{\underline{q} - u}{\alpha}\right) & , \underline{q} - \alpha \leqslant u \leqslant \underline{q} \\ 1 & , u \in \left[\underline{q}, \overline{q}\right] \\ R\left(\frac{u - \overline{q}}{\beta}\right) & , \overline{q} \leqslant u \leqslant \overline{q} + \beta \\ 0 & , \text{otherwise} \end{cases} \tag{5}$$

where $\left[\underline{q}, \overline{q}\right]$ is the peak of$A$; $\underline{q}$ and $\overline{q}$ are the lower and upper modal values; and$L, R : [0,1] \rightarrow [0,1]$, with $L(0) = R(0) = 1$ and $L(1) = R(1) = 0$ being nonincreasing, continuous mappings. In this study, the notation$A = \left(\underline{q}, \overline{q}, \alpha, \beta\right)_{LR}$. The variables in parentheses represent the lower limit value, upper limit value, left extension, and right extension of LR-type fuzzy numbers.

2.3. Credibility constraints

The fuzzy credibility constraint planning method is a mathematical algorithm used to resolve the uncertainty in system model data and the inability to obtain an exact distribution of random data. According to the concept of plausibility, the probability of a fuzzy event can be expressed as follows:

$$max \sum_{j=1}^{n} \widetilde{c}_j \cdot x_j \tag{6}$$

$$Cr\left\{ \sum_{j=1}^{n} \widetilde{a}_{ij} \cdot x_j \leqslant \widetilde{b}_i \right\} \geqslant \lambda_i, \quad (i = 1, \cdots, m) \tag{7}$$

$$x_j \geqslant 0, \quad (i = 1, \cdots, m) \tag{8}$$

where $x = (x_1, x_2, \cdots, x_n)$ is the nonfuzzy decision variable of the selected vector model; $\widetilde{c}_j$ is the coefficient in the objective function; and $\widetilde{a}_{ij}$ and $\widetilde{b}_i$ are the fuzzy coefficients in the constraint. Here, i is the number of constraints, and j is the number of variables. Eq. (6) is the optimization objective function, and Eq. (7) indicates that the confidence level of constraint $\sum_{j=1}^{n} \widetilde{a}_{ij} \cdot x_j \leqslant \widetilde{b}_i$ should be greater than or equal to the probabilityλ_i.

2.4. Multiobjective nonlinear optimization model based on left–right type fuzzy numbers and fuzzy credibility constraint planning

The steps required to solve the LR-FN-MONLP problem are as follows.

Step 1. The LR-FN-MONLP problem is modeled.

Step 2. LR-type fuzzy numbers are introduced to quantify the uncertain parameters.

Step 3. The affiliation function of each objective function is defined.

Step 4. The concepts of the possibilistic mean value and credibility measure are applied to transform the multiobjective planning model based on LR-type fuzzy numbers into a deterministic single-objective planning model.

$\widetilde{A}_{LR}$ can be transformed based on the crisp possibilistic mean value $(M\left(\widetilde{A}\right))$ as follows [20]:

$$M\left(\widetilde{A}\right) = \frac{\left(M^*\left(\widetilde{A}\right) + M_*\left(\widetilde{A}\right)\right)}{2} = \int_0^1 \rho\left(inf\widetilde{A}_\rho + sup\widetilde{A}_\rho\right) d\rho \tag{9}$$

where $M^*\left(\widetilde{A}\right)$ and $M_*\left(\widetilde{A}\right)$ are the upper and lower possibilistic mean values of$\widetilde{A}_{LR}$; ρ is a fuzzy level and can refer to the ρ-level cut for$\widetilde{A}_{LR}$, with$\rho \in [0,1]$; $inf\widetilde{A}_\rho$and $sup\widetilde{A}_\rho$ are the left and right extreme points, respectively.

Therefore, the possibilistic mean value can be obtained as follows:

$$\overline{M}\left(\widetilde{A}\right) = \frac{\underline{a} + \overline{a}}{2} + \frac{\beta - \alpha}{6} \tag{10}$$

Step 5. The uncertainty constraint with LR-type fuzzy numbers is converted into an equivalent deterministic form through plausibility constraints.

Liu et al. [21] defined the credibility measure Cr for real number λ and LR-fuzzy number $\overline{A}_{LR}$ with a membership function as follows:

$$Cr\left\{\widetilde{A}^* r\right\} = \frac{1}{2}\left(Pos\left\{\widetilde{A}^* r\right\} + Nec\left\{\widetilde{A}^* r\right\}\right) \tag{11}$$

If the corresponding ρ-critical values are greater than 0.5, then the fuzzy constraints can be transformed into equivalent crisp constraints as follows:

$$Cr\left\{\widetilde{A} \leqslant r\right\} \geqslant \rho \quad \Leftrightarrow \quad r \geqslant (2 - 2\rho)\overline{a} + (2\rho - 1)(\overline{a} + \beta) \tag{12}$$

$$Cr\left\{\widetilde{A} \geqslant r\right\} \geqslant \rho \quad \Leftrightarrow \quad r \leqslant (2\rho - 1)(\underline{\alpha} - \alpha) + (2 - 2\rho)\underline{\alpha} \tag{13}$$

Step 6. The transformed model is solved for different confidence probabilities, and a solution is generated.

3. Model development

In a region dominated by cultivation, a WEFN system is established to achieve conversions and trade-offs among the light use efficiency, quantity of biomass electrical energy, and quantity of hydroelectric energy through the dynamic regulation of the main driving elements of the WEFN, water resources, the cultivation structure, and energy to promote regional sustainable development. Fig. 1 shows the relationship between regulated resources and objectives in the WEFN.

The LR-FN-MONLP model is constructed considering three elements: objective functions, constraints and decision variables. The objective functions involve biomass electrical energy maximization, light use efficiency maximization, and hydroelectric energy minimization. The constraints include surface water availability, groundwater availability, the water demand, the water balance, electrical energy availability, land use and nonnegative constraints. The decision variables include surface water irrigation quotas, groundwater irrigation quotas; water cycle elements for different growth stages in various subareas with different crops; surface water availability, groundwater availability, and power availability in different subareas; and ares in different subareas with various crops.

The parameters involved in the decision-making process, such as the maximum light use efficiency, crop yield, water pump efficiency, surface water availability, and crop water demand, are subjective and uncertain due to socioeconomic activities and fluctuations in natural conditions, and they are thus defined as LR-type fuzzy numbers. The model constraints are expressed as credibility constraints due to data uncertainty. The framework of the model is shown in Fig. 2.

3.1. Notations

To clearly understand the model parameters and variables, their meanings are provided in Table 1.

3.2. Objective function

The objective functions of the constructed model involve maximizing biomass electrical energy, maximizing light energy utilization, and minimizing hydroelectric energy. A tradeoff among the three objectives is achieved by synergistically optimizing agricultural resource utilization, including water resources, land resources and energy. The specific expressions of the objective functions are as follows.

3.2.1. Biomass electrical energy maximization

Bioenergy is the energy provided by living plants in nature, which use biomass as a medium to store solar energy; additionally, biomass is a renewable energy source, an important link between energy, food and water in agricultural WEFN, and the most direct index for bioenergy potential assessment. Straw resulting from crop harvesting can be employed to produce biomass energy, which can be further converted into electrical energy. Increasing biomass electrical energy production allows the generated electrical energy to be applied in various other areas or in the next stage of crop production for waste utilization, and this approach promotes green and efficient agriculture [22]. The expression of this objective function is as follows [23]:

$$maxf^{BIOE} = \sum_{d=1}^{D}\sum_{c=1}^{C} A_{dc}\cdot\widetilde{Y}_{dc}\cdot\alpha_c\cdot\beta_c\cdot\gamma\cdot\delta_c\cdot\left[\frac{HHV_c\cdot eff\cdot\rho_{combustion}}{3.6}+\frac{HHV_c\cdot eff_{thermal}\cdot eff_{wtoE}\cdot\rho_{gasification}}{3.6}\right] \tag{14}$$

where $\sum_{d=1}^{D}\sum_{c=1}^{C} A_{dc}\cdot\widetilde{Y}_{dc}\cdot\alpha_c\cdot\beta_c\cdot\gamma\cdot\delta_c$ denotes the biomass output (kg), $\frac{HHV_c\cdot eff\cdot\rho_{combustion}}{3.6}$ denotes the fraction of the total energy contained in the feedstock used to generate electricity through combustion (kW·h/kg), and $\frac{HHV_c\cdot eff_{thermal}\cdot eff_{wtoE}\cdot\rho_{gasification}}{3.6}$ denotes the fraction of electrical energy

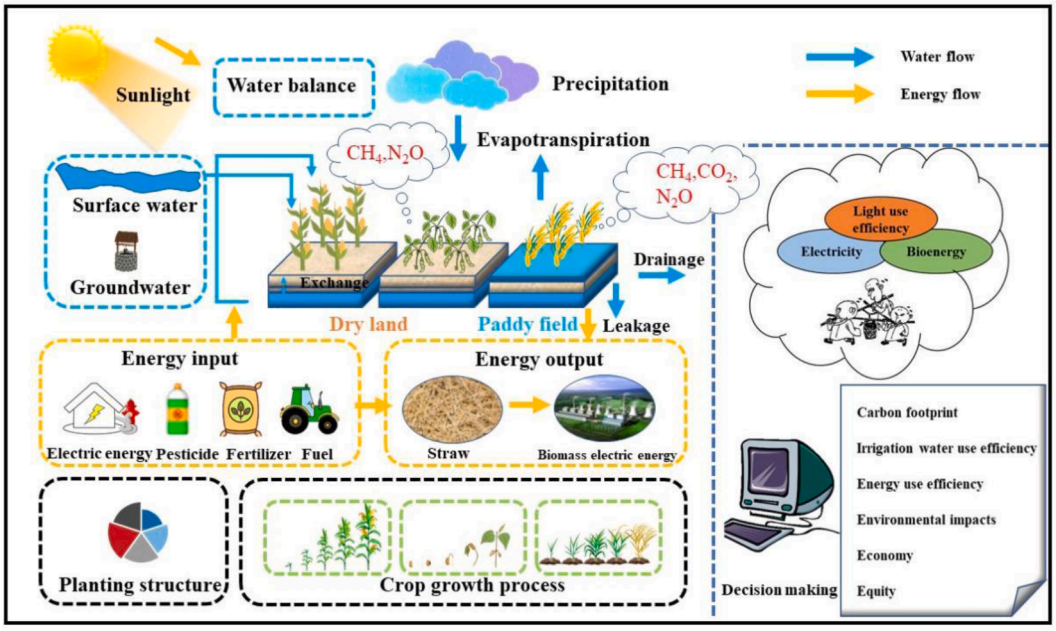

Fig. 1. WEFN in an agricultural system.

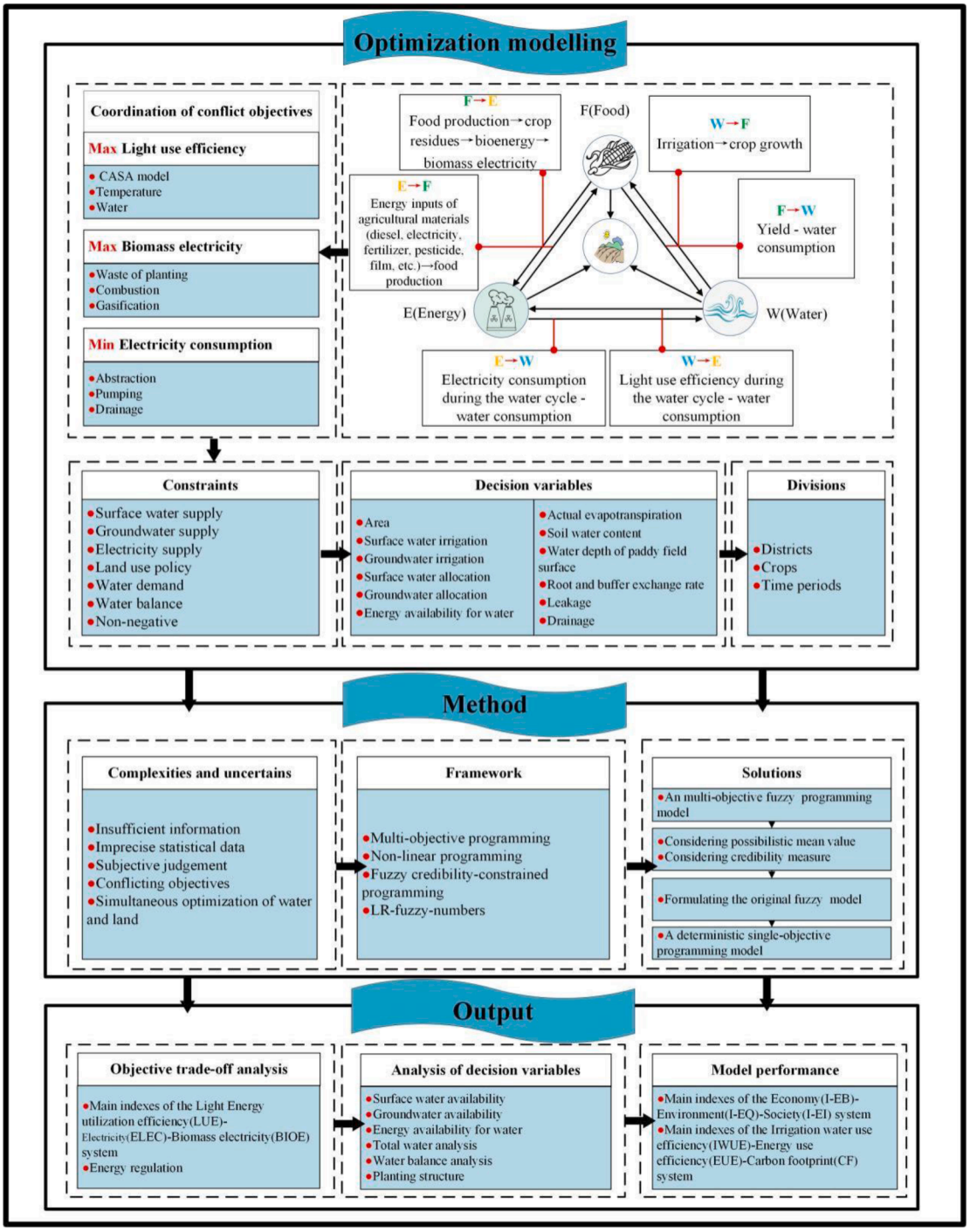

Fig. 2. Framework of the model.

(kW·h/kg) generated via gas combustion in an internal combustion engine.

3.2.2. *Light use efficiency maximization*

The light use efficiency, which is maximized as the main objective of the model, refers to the conversion of photosynthetically active radiation absorbed by vegetation into organic carbon, thus reflecting the ability of plants to convert light into chemical energy. Light use efficiency enhancement is beneficial for crops to increase biomass and thus yield. In this study, the effects of temperature and moisture on the light use efficiency were considered based on the modified Carnegie-Ames-Stanford approach (CASA) model proposed in Potter et al. [24], and the corresponding objective function can be expressed as follows:

$$maxf^{LUE} = \frac{\sum_{d=1}^{D}\sum_{c=1}^{C}\sum_{t=1}^{T} T_{dct}^{\varepsilon 1} \cdot T_{dct}^{\varepsilon 2} \cdot W_{dct}^{\varepsilon} \cdot \tilde{e}_{dct}^{*}}{SU} \tag{15}$$

Table 1
Significance of the model parameters and variables.

Indices	
c	Crop index
d	District index
t	Period index
gro	Superscript for groundwater
sur	Superscript for surface water
max	Superscript for the maximum value
min	Superscript for the minimum value
Symbols for the objective functions	
f^{BIOE}	Objective function of biomass electrical energy (kW·h)
f^{ELEC}	Objective function of hydroelectric energy (kW·h)
f^{LUE}	Objective function of the light use efficiency (g C/MJ)
Parameters	
α_c	Straw-grain ratio for crop c
β_c	Straw collection coefficient for crop c
γ	Coefficient of new energy availability
δ_c	Conversion ratio from the residue of crop c to the standard coal equivalent
$\rho_{combustion}$	Combustion coefficient
$\rho_{gasification}$	Gasification coefficient
η^{sur}	Utilization coefficient for surface irrigation
η^{gro}	Utilization coefficient for well irrigation
$\widetilde{\mu}^{sur}$	Efficiency of surface water abstraction (LR-FN)
$\widetilde{\mu}^{pump}$	Pump efficiency (LR-FN)
μ^{motor}	Motor efficiency
$\widetilde{\mu}^{dra}$	Drainage efficiency (LR-FN)
$\widetilde{\varepsilon}^{*}_{dct}$	Maximum light use efficiency for crop c in subarea d during period t (g C/MJ) (LR-FN)
A^{min}_{dc}	Lower limit of land availability for crop c in subarea d (ha)
A^{max}_{dc}	Upper limit of land availability for crop c in subarea d (ha)
$\widetilde{D}^{min}_{dct}$	Minimum water demand (m^3) (LR-FN)
DM_c	Drainage modulus for crop c (m^3/d/ha)
eff	Electrical efficiency of an incineration plant
$eff_{thermal}$	Thermal efficiency of an internal combustion engine
eff_{wtoE}	Efficiency of the conversion of mechanical work to electricity
ECI^{sur}	Electricity for irrigation with surface water (kW·h)
ECI^{gro}	Electricity for irrigation with groundwater (kW·h)
ECD	Electricity for drainage (kW·h)
EWA	Total energy availability for water (kW·h)
$ET_{0,dct}$	Reference evapotranspiration for crop c in subarea d during period t (m^3/ha)
H^{lift}	Pumping lift head (m)
H^{nop}	Nominal operating pressure (m)
$H^{lossess}$	Head loss (m)
HD_d	Drainage head in subarea d (m)
HHV_c	Higher heating value of crop c (MJ/kg)
HI^{sur}	Hydraulic head of surface water (m)
P_{dct}	Effective precipitation for crop c in subarea d during period t (m^3/ha)
SU	Product of the number of different division quantities
T^{e1}_{dct}	Temperature stress factor 1 for crop c in subarea d during period$t$
T^{e2}_{dct}	Temperature stress factor 2 for crop c in subarea d during period$t$
T^{opt}_{dct}	Optimum temperature for crop c in subarea d during period t (℃)
TW_{dct}	Average temperature for crop c in subarea d during period t (℃)
$\widetilde{TWS}^{sur}$	Total surface water supply (m^3) (LR-FN)
TWS^{gro}	Total groundwater supply (m^3)
TS_c	Number of drainage days for crop c (d)
W^{e}_{dct}	Water stress factor for crop c in subarea d during period$t$
$\widetilde{Y}_{dc}$	Yield per unit area of crop c in subarea d (kg/ha) (LR-FN)
Decision variables	
A_{dc}	Irrigation area of crop c in subarea d (ha)
D_{dct}	Drainage for crop c in subarea d during period t (m^3/ha)
ESI_d	Energy availability for water use in subarea d (kW·h)
$ET_{a,dct}$	Actual evapotranspiration for crop c in subarea d during period t (m^3/ha)
ET^{g}_{dct}	Root and buffer exchange rate for crop c in subarea d during period t (m^3/ha)
H_{dct}	Water depth at the paddy field surface for crop c in subarea d during period t (m^3/ha)
IQ^{sur}_{dct}	Surface water irrigation for crop c in subarea d during period t (m^3/ha)
IQ^{gro}_{dct}	Groundwater irrigation for crop c in subarea d during period t (m^3/ha)
L_{dct}	Leakage for crop c in subarea d during period t (m^3/ha)
W_{dct}	Soil moisture content for crop c in subarea d during period t (m^3/ha)
WS^{sur}_{d}	Surface water availability in subarea d (m^3)
WS^{gro}_{d}	Groundwater availability for irrigated agriculture in subarea d (m^3)

(1) Calculation of temperature stress factors.

$T_{dct}^{\varepsilon 1}$ and $T_{dct}^{\varepsilon 2}$ are temperature stress factors, which represent the changes in light use efficiency due to photosynthesis inhibition and respiration promotion during plant growth in low- and high-temperature environments, respectively; the specific equations for these temperature stress factors are as follows:

$$T_{dct}^{\varepsilon 1} = 0.8 + 0.002 \cdot T_{dct}^{opt} - 0.0005 \cdot \left(T_{dct}^{opt}\right)^2 \tag{16}$$

$$T_{dct}^{\varepsilon 2} = \frac{1.184}{\left\{1 + exp\left[0.2 \cdot \left(T_{dct}^{opt} - 10 - TW_{dct}\right)\right]\right\} \cdot \left\{1 + exp\left[0.3 \cdot \left(-T_{dct}^{opt} - 10 + TW_{dct}\right)\right]\right\}} \tag{17}$$

(2) Calculation of water stress factors.

W_{dct}^{ε} represents the stress effect of water on plant growth in the CASA model, thus reflecting the magnitude of the effect of different hydrological and environmental conditions on plant photosynthesis; notably, the value of this variable ranges from 0.5 to 1. In the case of extreme drought, W_{dct}^{ε} tends to approach 0.5. The wetter the environment is, the larger the W_{dct}^{ε} value, and the maximum value can approach 1. The expression is as follows:

$$W_{dct}^{\varepsilon} = 0.5 \cdot \frac{ET_{a,dct}}{ET_{0,dct}} + 0.5 \tag{18}$$

3.2.3. Hydroelectric energy minimization

Electricity consumption occurs during surface water extraction and groundwater pumping and drainage, and the corresponding functional expression is directly related to the pumping head. To pump water from aquifers, the pumping head, the rated operating pressure and friction losses should be considered. A reduction in the required hydraulic electrical energy can reduce energy consumption, as denoted by the following expression [25]:

$$minf^{ELEC} = ECI^{sur} + ECI^{gro} + ECD \tag{19}$$

$$ECI^{sur} = \left[\frac{HI^{sur}}{102 \times 3.6 \cdot \widetilde{\mu}^{sur}} \left(\sum_{d=1}^{D}\sum_{c=1}^{C}\sum_{t=1}^{T} IQ_{dct}^{sur} \cdot A_{dc}\right)\right] \tag{20}$$

$$ECI^{gro} = \left[\frac{H^{lift} + H^{nop} + H^{lossess}}{102 \times 3.6 \cdot \widetilde{\mu}^{pump} \cdot \mu^{motor}} \left(\sum_{d=1}^{D}\sum_{c=1}^{C}\sum_{t=1}^{T} IQ_{dct}^{gro} \cdot A_{dc}\right)\right] \tag{21}$$

$$ECD = \left[\sum_{d=1}^{D}\sum_{t=1}^{T} \frac{HD_d}{102 \times 3.6 \cdot \widetilde{\mu}_d^{dra}} \left(\sum_{c=1}^{C} DM_c \cdot TS_c\right) \cdot A_{dc}\right] \tag{22}$$

3.3. Constraints

The above objective function is conditioned by the following seven conditions:

(1) Surface water availability constraint

The surface water allocation amounts at all growth stages for the different crops should not be greater than the surface water supply in each subarea. Usually, the total surface water available in an area is derived from runoff but is less than the runoff volume (because of the requirement to retain ecological runoff from rivers). In this constraint, $\widetilde{TWS}^{sur}$ is the total surface water supply. The total surface water supply always varies due to precipitation, climate, temperature and other factors, and this parameter is thus defined as an LR-type fuzzy number, and this constraint can be expressed as:

$$\sum_{c=1}^{C}\sum_{t=1}^{T} A_{dc} \cdot IQ_{dct}^{sur} \leqslant WS_d^{sur} \cdot \eta^{sur} \qquad \forall d \tag{23}$$

$$Cr\left(\sum_{d=1}^{D} WS_d^{sur} \leqslant \widetilde{TWS}^{sur}\right) \geqslant \tau \tag{24}$$

(2) Groundwater availability constraint.

Similar to surface water, the groundwater allocation amounts at all growth stages for the different crops should not exceed the groundwater supply in each subzone. The available groundwater supply in all subareas should not be greater than the extractable groundwater amount in these areas. This constraint can be expressed as follows:

$$\sum_{c=1}^{C}\sum_{t=1}^{T} A_{dc} \cdot IQ_{dc}^{gro} \leqslant WS_d^{gro} \cdot \eta^{gro} \qquad \forall d \tag{25}$$

$$\sum_{d=1}^{D} WS_d^{gro} \leqslant TWS^{gro} \tag{26}$$

(3) Water demand constraint

The water demand of the different crops at the various growth stages in the different subareas should be no greater than the sum of the surface water and groundwater irrigation quotas of the different crops at the various growth stages in the different subareas, which is defined as an LR-type fuzzy number due to the influence of environmental fluctuations and other factors, and the constraint is expressed as follows:

$$Cr\left(IQ_{dct}^{sur} + IQ_{dct}^{gro} \geqslant \widetilde{D_{dct}^{min}}\right) \geqslant \varsigma \ \forall d, c, t \tag{27}$$

(4) Water balance constraint.

The water balance constraint describes the changes in water depth (paddy fields) or soil water content (dry fields) when considering the recharge and discharge processes in farmlands, reflecting the dynamics and continuity of water changes at the different stages of crop fertility. The expression of this constraint is as follows:

Water balance constraint for irrigated fields:

$$ET_{a,dct} = H_{dct} - H_{dc,t+1} + P_{dct} + IQ_{dct}^{sur} + IQ_{dct}^{gro} - L_{dct} - D_{dct} \qquad \forall d, c = 1, t \tag{28}$$

where the drainage volume is related to the water depth at the paddy field surface and can be expressed with the following equation:

$$D_{dct} = \begin{cases} 0 & H_{dct} \leqslant H_s \\ H_{dct} - H_s & H_{dct} > H_s \end{cases} \quad \forall d, c = 1, t \tag{29}$$

The water depth at the surface of a paddy field should be smaller than the maximum depth of the water layer:

$$H_{dct} \leqslant H_{dct}^{max} \quad \forall d, c = 1, t \tag{30}$$

Dryland water balance constraints:

$$ET_{a,dct} = W_{dct} - W_{dc,t+1} + P_{dct} + IQ_{dct}^{sur} + IQ_{dct}^{gro} + ET_{dct}^{g} \qquad \forall d, c = 2, 3, t \tag{31}$$

The dryland soil moisture content should vary between the minimum and maximum soil moisture contents, as follows:

$$W_{dct}^{min} \leqslant W_{dct} \leqslant W_{dct}^{max} \quad \forall d, c = 2, 3, t \tag{32}$$

(5) Electrical energy availability constraint

In irrigated agricultural systems, where energy is mainly employed

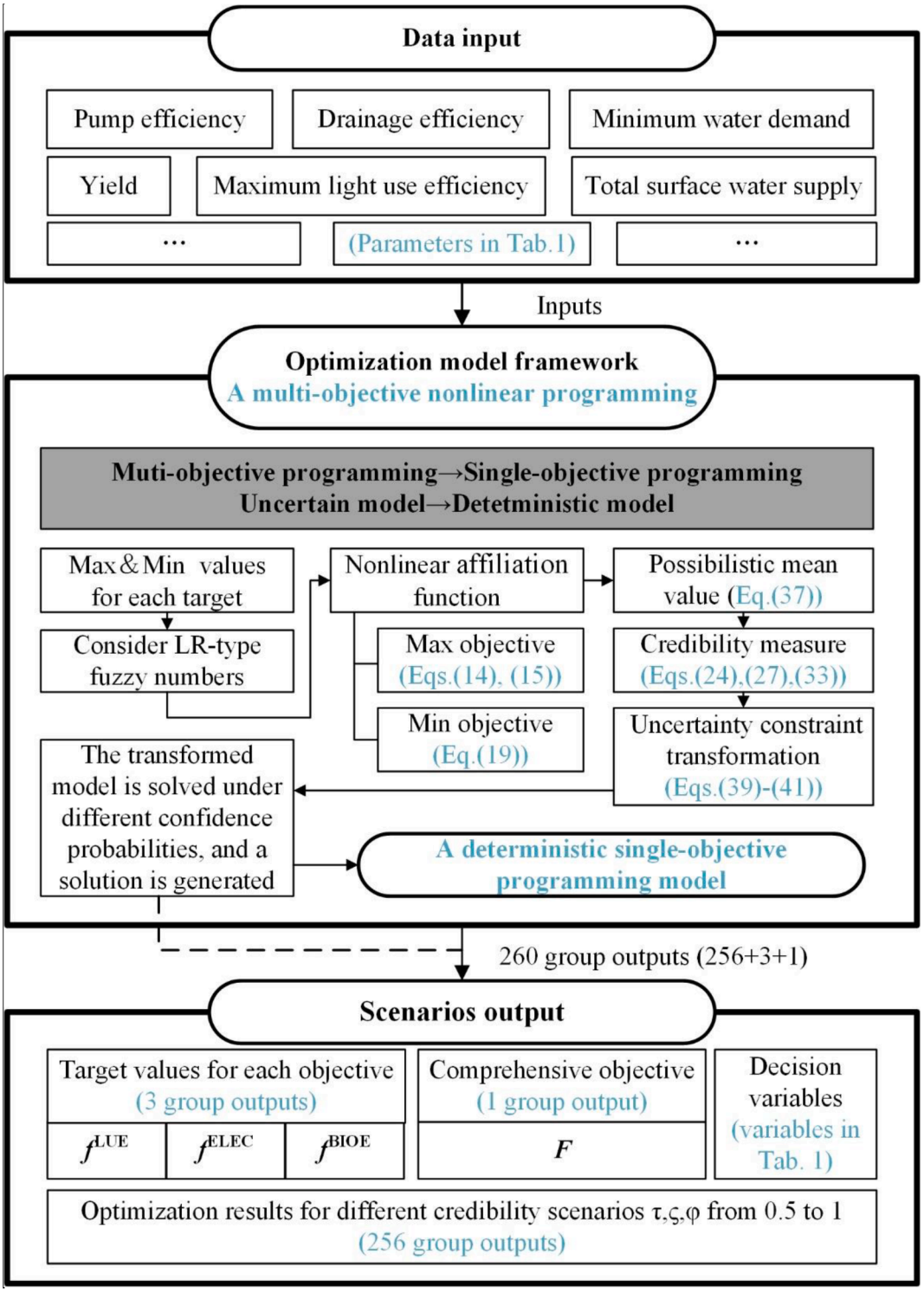

Fig. 3. Solution method of the optimization model.

for surface water extraction, groundwater pumping and drainage, the resultant electricity consumption should not exceed the allowable quantity and total energy availability in each district. The expression is optimized for agricultural energy. This constraint can be expressed as follows:

$$Cr\left\{\sum_{c=1}^{C}\sum_{t=1}^{T}A_{dc}\cdot\left[\left(\frac{H^{Lift}+H^{nop}+H^{lossess}}{102\times 3.6\cdot\widetilde{\mu}^{pump}\cdot\mu^{motor}}\cdot IQ_{dct}^{gro}\right)+\left(\frac{HD_d}{102\times 3.6\cdot\widetilde{\mu}_d^{dra}}\cdot DM_c\cdot TS_c\right)+\left(\frac{HI^{sur}}{102\times 3.6\cdot\widetilde{\mu}^{sur}}\cdot IQ_{dct}^{sur}\right)\right]\leqslant ESI_d\right\}\geqslant\phi\ \forall d \tag{33}$$

$$\sum_{d=1}^{D}ESI_d\leqslant EWA \tag{34}$$

(6) Land use constraint

For each crop in the different subareas and for each crop type in all subareas, the lower and upper limits of the irrigated area should be considered based on food requirements and major crop production practices. This constraint can be expressed as follows:

$$A_{dc}^{min}\leqslant A_{dc}\leqslant A_{dc}^{max}\quad\forall d,c \tag{35}$$

(7) Nonnegative constraint

The decision variables should be nonnegative.

$$IQ_{dct}^{sur},IQ_{dct}^{gro},A_{dc},WS_d^{sur},WS_d^{gro},ESI_d,ET_{a,dct},H_{dct},L_{dct},D_{dct},W_{dct},ET_{dct}^{g}\geqslant 0 \tag{36}$$

3.4. Model solution

A multienergy coordination model for agricultural WEFN with the proposed LR-FN-MONLP framework was developed based on the information presented in sections 3.1 to 3.3. Based on the solution steps of LR-FN-MONLP (section 2.4), the key to solving the model is to transform the uncertain multiobjective programming model into a deterministic single-objective programming model based on the concepts of the possibilistic mean value and credibility measure. Here, three objectives are considered equally important. The final transformed model is expressed as follows, and the specific transformation processes are shown in the Supplementary Materials.

$$maxF \tag{37}$$

where F is the weighted possibilistic mean value of the objective function,$\widetilde{F}=[\underline{A},\overline{R},M,N]_{LR}$, and is calculated as follows:

$$F=\frac{\underline{A}+\overline{R}}{2}+\frac{N-M}{6} \tag{38}$$

Specific expressions of$\underline{A}$,$\overline{R}$,M, and N are provided in the Supplementary Materials.

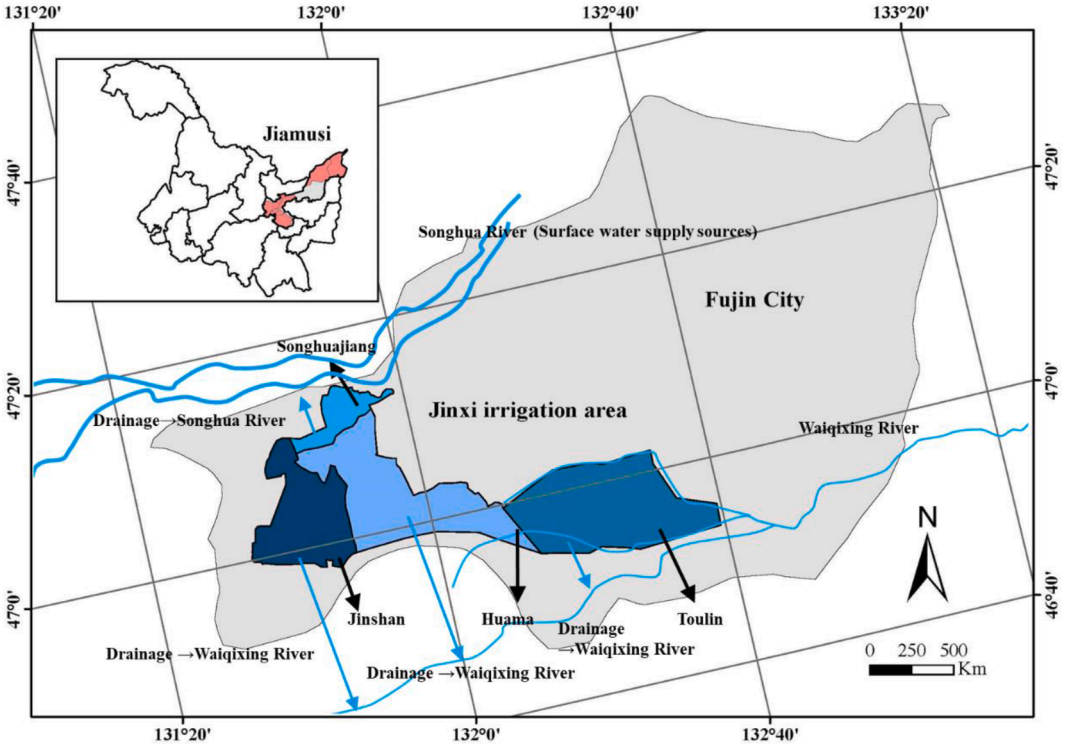

Fig. 4. Study area.

Constraints:

$$\sum_{d=1}^{D} WS_d^{sur} \leqslant [(2\tau-1)(\underline{TWS}^{sur} - \alpha\underline{TWS}^{sur}) + (2-2\tau)\underline{TWS}^{sur}] \quad \forall d \tag{39}$$

$$IQ_{dct}^{sur} + IQ_{dct}^{gro} \geqslant (2-2\varsigma)\overline{D}_{dct}^{min} + (2\varsigma-1)(\overline{D}_{dct}^{min} + \beta D_{dct}^{min}) \quad \forall d,c,t \tag{40}$$

$$\sum_{c=1}^{C} A_{dc} \cdot \left\{ \begin{array}{l} \left[(2-2\phi)\cdot\dfrac{1}{\underline{\mu}^{sur}} + (2\phi-1)\left(\dfrac{1}{\underline{\mu}^{sur}} + \dfrac{1}{\alpha\mu^{sur}}\right)\right] \cdot IQ_{dct}^{sur} \cdot \dfrac{H^{sur}}{102\times 3.6} \\ + \left[(2-2\phi)\cdot\dfrac{1}{\underline{\mu}^{pump}} + (2\phi-1)\left(\dfrac{1}{\underline{\mu}^{pump}} + \dfrac{1}{\alpha\mu^{pump}}\right)\right] \\ \cdot IQ_{dct}^{gro} \cdot \dfrac{H^{lift} + H^{nop} + H^{lossess}}{102\times 3.6\cdot\mu^{motor}} \\ + \left[(2-2\phi)\cdot\dfrac{1}{\underline{\mu}^{d}} + (2\phi-1)\left(\dfrac{1}{\underline{\mu}^{d}} + \dfrac{1}{\alpha\mu^{d}}\right)\right] \cdot DM_c \cdot TS_c \cdot \dfrac{HD}{102\times 3.6} \end{array} \right\} \leqslant ECI_d \quad \forall d \tag{41}$$

where (39), (40), and (41) denote the transformations of fuzzy constraints (24), (27), and (33), respectively, into equivalent exact constraints considering plausibility constraints. where τ, ς and ϕ denote the variables determined by the decision maker to satisfy the probability chance constraint at the lowest confidence level, and these variables should be provided at a confidence level higher than or equal to 0.5, i.e.,$\tau, \varsigma, \phi \geqslant 0.5$. The remaining constraints are the same as those in Eqs. (23), (25), (26), (28), (29), (30), (31), (32), (34), (35), and (36).

Based on the input parameters in Table 1, the transformed model can be coded in a software package to solve the optimization model and then output the values of decision variables (i.e., the 12 decision variables in Table 1). In this study, the model is programmed using LINGO software, and the data are imported and exported using Excel. For each fuzzy scenario (a certain confidence level), three LINGO procedures related to the affiliation function of each objective function are needed to help transform the multiobjective programming problem into a single-objective programming problem. Together with the combined model procedure based on the above transformed model, there are a total of 4 LINGO procedures, and each procedure takes approximately one minute. Therefore, for each fuzzy scenario, 4 min are needed to obtain the final solution. In this study, 256 fuzzy scenarios are considered, so the total solution time is 260 min. The specific solution flow chart for the model is shown in Fig. 3.

Table 2
Relevant parameters for the different crops.

Parameters	Parameter	Unit	Crops		
			Rice	Corn	Soybean
Straw-grain ratio	α_c	dimensionless	0.98	1	1.36
Collectable coefficient of straw	β_c	dimensionless	0.72	0.87	0.56
Higher heating value	HHV_c	MJ/kg	18.8	19.2	16.2
Conversion ratio stands for the ratio from the residue	δ_c	dimensionless	0.429	0.529	0.543
Price of crop	P_c	Yuan/kg	3.16	2.25	5.4
Fertilizer	ε_c^{fer}	Yuan/ha	885	800.55	645.3
Pesticide	ε_c^{pes}	Yuan/ha	289.2	148.2	141.6
Agricultural machinery	ε_c^{mac}	Yuan/ha	1566.3	973.05	846.9
Seed	ε_c^{seed}	Yuan/ha	320.4	350.85	476.7
Labor	ε_c^{lab}	Yuan/ha	1361.4	1043.7	311.55
Agricultural film	ε_c^{film}	Yuan/ha	2.1	2.1	2.1
Drainage modulus	DM_c	m^3/d/ha	80.352	67.392	67.392
Drainage duration	TS_c	d	4	2	2

4. Model application

The model application involves two steps: 1. Selection of the study area and 2. Data collection.

4.1. Study area

The study area is located in the Jinxi Irrigation District in Fujin city, Heilongjiang Province, Northeast China. The longitude of this area ranges from 131°30′ to 132°37′E, and the latitude ranges from 46°48′ to 47°14′N. The study area has a temperate continental climate (Fig. 4). The Jinxi Irrigation District is located on the right bank and in the lower reaches of the main channel of the Songhuajiang River, with a cultivated land area covering 1.011×10^5 ha. The Jinxi Irrigation District contains four subareas: the Jinshan, Songhuajiang, Toulin and Huama subareas. Irrigated agriculture is the largest water use type in the Jinxi Irrigation District, accounting for nearly 90% of the total water consumption. The average annual precipitation and evaporation are 542 and 720 mm, respectively. The Jinxi Irrigation District is a dual-irrigation district involving canals and wells, and the Songhua River is the main source of the surface water supply. The rapid pace of agricultural development in the Jinxi Irrigation District has led to groundwater overdraft due to a lack of water diversion and pumping projects. To mitigate the imbalance in water utilization, a pumping station at the head of the canal and drainage pumping stations were established. There are six drainage pumping stations across the Jinxi Irrigation District, including the Shanxi, Huama, Duijin, Shuangyushu, Toulin and Erlin drainage pumping stations. Water originating from the Songhuajiang subarea is discharged directly into the Songhua River, and water originating from the Jinshan, Huama and Toulin subareas is eventually discharged into the Waiqixing River. The Jinxi Irrigation District is an important food production base in Heilongjiang Province, China, with rice, corn, soybeans, vegetables and melons as the main crops. Among these crops, rice, corn and soybean food crops have covered nearly 90% of the total arable land area over the past five years. Therefore, these three food crops were selected for further analysis in this study.

4.2. Data collection

The data required for LR-FN-MONLP model construction are used to

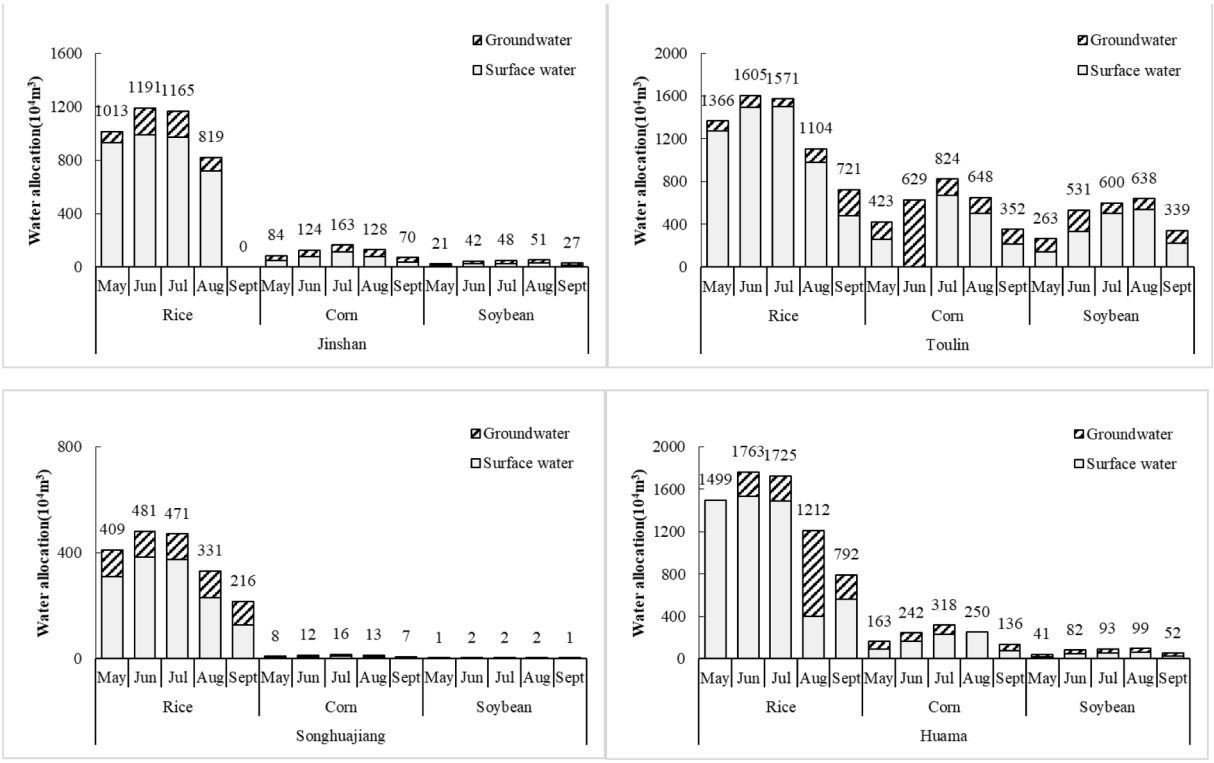

Fig. 5. Water allocation in the different subareas for various crops and growth stages.

establish meteorological, hydrological and agricultural production-related parameters and coefficients. These data were mainly obtained from the Fujin City Statistical Bulletin, the Fujin City Statistical Yearbook, the China Meteorological Data Network (https://data.cma.cn/), government reports and published references. Hydrological data included the crop water demand and water supply, effective rainfall, crop evapotranspiration, the field water depth, drainage and seepage in each stage of paddy field growth, the soil water content in dry fields, and the exchange rate between root and buffer zones. The light use efficiency data required for the improved CASA model mainly included maximum light use efficiency [26], temperature and moisture data [27]. The required biomass electrical energy data mainly included the straw-to-grain ratio, straw collection coefficient, higher heating value, discount coal coefficient, gasification efficiency of internal combustion engines, and combustion efficiency of internal combustion engines. The required hydroelectric energy data primarily included the discharge modulus, discharge period, and water pump efficiency.

The socioeconomic and environmental data mainly included the market price, the water price, the water resource use efficiency, land resource data, fertilizer use information, population- and crop-related coefficients, energy utilization information, the carbon footprint, and irrigation water use efficiency data, which can be used to determine most agricultural carbon emission sources and the related coefficients [28], surface water loss, groundwater leaching, and energy coefficients for agricultural production [29]. Certain relevant parameters for the different crops are listed in Table 2, and other related data are listed in the Supplementary Materials.

In Table 2, the biomass energy conversion correlation coefficient is mainly from [30], the agricultural parameter prices are mainly from the "*Agricultural Product Price Information Network of Heilongjiang Province*" and the statistical yearbook of Fujin city. The drainage parameters were obtained from the "*Engineering Feasibility Study Report of Jinxi Irrigation District*".

5. Results analysis and discussion

The results analysis and discussion concentrates on agricultural resources regulation, multi-energy tradeoff and model performance.

5.1. Water quantity regulation and control

Figure 5 shows the water allocation schemes for the different crops in the various subareas and all crop growth stages. Fig. 5 reveals that for rice crops, the allocated irrigated area in the Songhuajiang subarea is small, which results in a much smaller water allocation amount in the Songhuajiang subarea than in the other three subareas. For corn and soybean crops, the water allocation in the Toulin subarea is much larger than that in the other three subareas; moreover, the water allocation in the Jinshan and Huama subareas is moderate, and the water allocation amount in the Songhuajiang subarea is the smallest, as determined by the allocated irrigated area. Surface water and groundwater are more evenly distributed. In general, surface water is the main water supply source, and the ratio of surface water to groundwater use is 7:2.

The surface water and groundwater availability proportions in the different subareas are as follows: the surface water availability in the Jinshan subarea reaches 8843.52 $\times$ 10^4 m^3 (20.58%), that in the Toulin subarea reaches 18203.37 $\times$ 10^4 m^3 (42.36%), that in the Songhuajiang subarea reaches 2915.30 $\times$ 10^4 m^3 (6.78%), and that in the Huama subarea reaches 13007.51 $\times$ 10^4 m^3 (30.27%). The available groundwater supply is 1246.97 $\times$ 10^4 m^3 (17.52%) in the Jinshan subarea, 2956.49 $\times$ 10^4 m^3 (41.54%) in the Toulin subarea, 605.25 $\times$ 10^4 m^3 (8.50%) in the Songhuajiang subarea and 2308.06 $\times$ 10^4 m^3 (32.43%) in the Huama subarea. The total water distribution is the highest in the Toulin subarea, followed by the Huama subarea and finally the Jinshan and Songhuajiang subareas. In terms of the surface water and groundwater distributions, the water distribution proportion in each subarea does not vary greatly, and the largest change is only 3.06% (the Jinshan subarea).

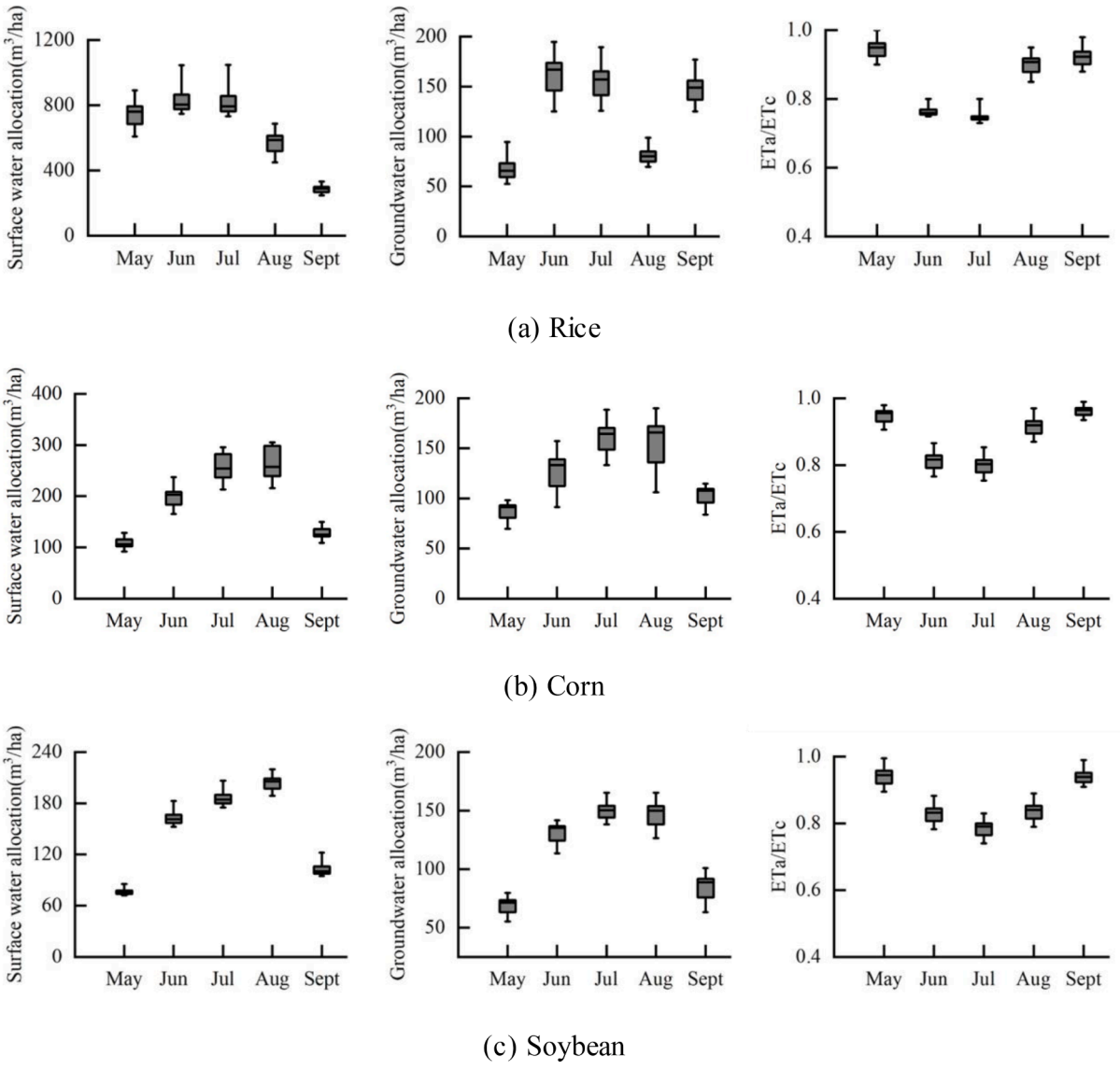

Fig. 6. Variation of each water cycle element of different crops at each growth stage.

Surface water irrigation, groundwater irrigation and precipitation are the main sources of crop recharge in the field. Fig. 6 shows the variation in each water quantity element in each growth stage for the different crops. Optimization is based on the number of growth stage days, the crop water demand, precipitation, water deficit sensitivity, and the water allocation objectives. Based on the water balance, the crop water consumption in each growth stage can be obtained, and the ratio of water consumption to the water demand (relative water consumption) can be used to determine the water deficit in each growth stage and the corresponding contribution to the yield. For rice crops, the total water allocation amount was largest in June and July, followed by May, with comparable water allocation amounts in August and September. The water allocation percentages from May to September were [21.45% ± 2.83%], [25.21% ± 2.30%], [24.67% ± 2.44%], [17.33% ± 1.80%], and [11.33% ± 0.82%]. The distribution ratios of surface water, groundwater and precipitation from May to September were 0.49:0.04:0.46, 0.49:0.10:0.41, 0.43:0.09:0.48, 0.44:0.06:0.50, and 0.24:0.12:0.63, respectively. The surface water and groundwater allocation ratios in May, June, July, and August basically remained the same, but they were lower in September. Although the total water allocation amounts in June and July were larger than those in May and September, the water consumption in the former months was significantly lower. This difference was particularly notable in July and is directly related to the insufficient total water supply in the irrigation area; thus, the corresponding growth stage was the most sensitive in regard to water shortages. More water should be preferentially allocated in July if more investment is made to replenish water. In the case of corn crops, the total water allocation amount was largest in July and August, followed by June, with comparable water allocation amounts in May and September. The water allocation percentages from May to September were [12.29% ± 0.81%], [20.89% ± 1.55%], [26.05% ± 2.86%], [26.31% ± 3.68%], and [14.46% ± 0.92%]. The distribution ratios of surface water, groundwater and precipitation from May to September were 0.12:0.10:0.78, 0.20:0.13:0.67, 0.20:0.13:0.68, 0.24:0.15:0.61, and 0.13:0.11:0.76, respectively. The surface water and groundwater allocation ratios in June, July and August were similar, the surface water and groundwater allocation ratios in May and September were comparable, and water consumption in June and July was low. These results indicate that June and July are critical periods for corn irrigation and that an adequate water supply should be maintained. For soybean crops, the total water allocation amount was largest in July and August, followed by June, with comparable water allocation amounts in May and September. The water allocation percentages from May to September were [11.09% ± 0.63%], [22.41% ± 1.56%], [25.30% ±

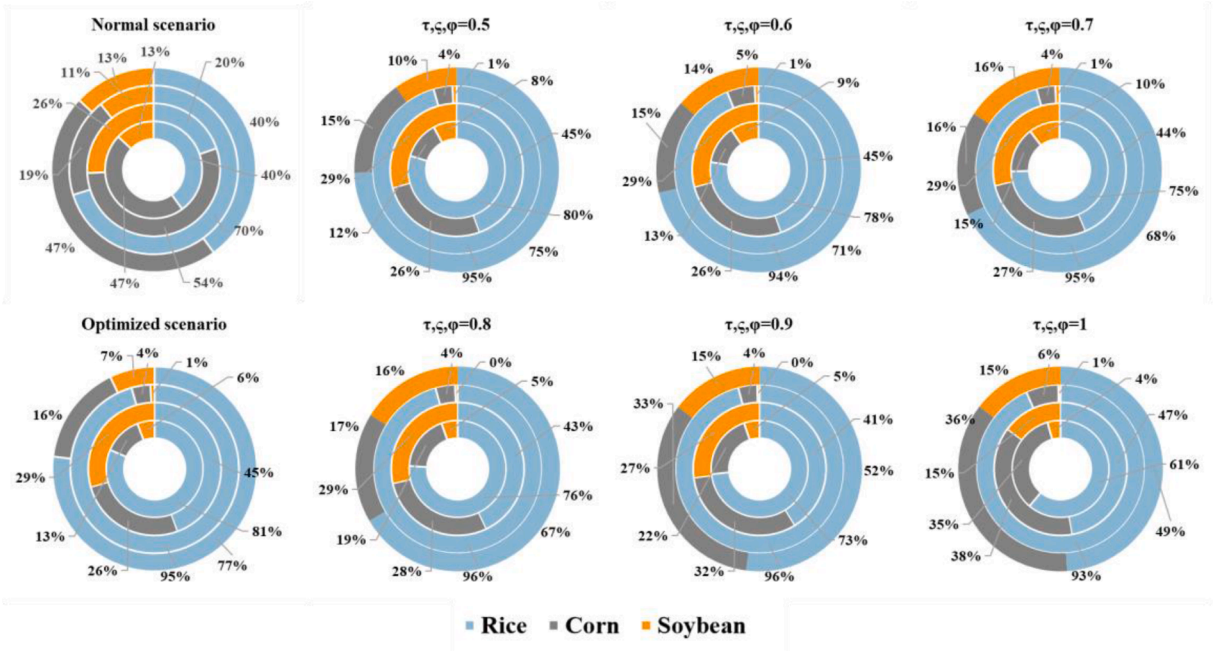

Fig. 7. Proportion of the planted area of the different crops in the various subareas under different scenarios.

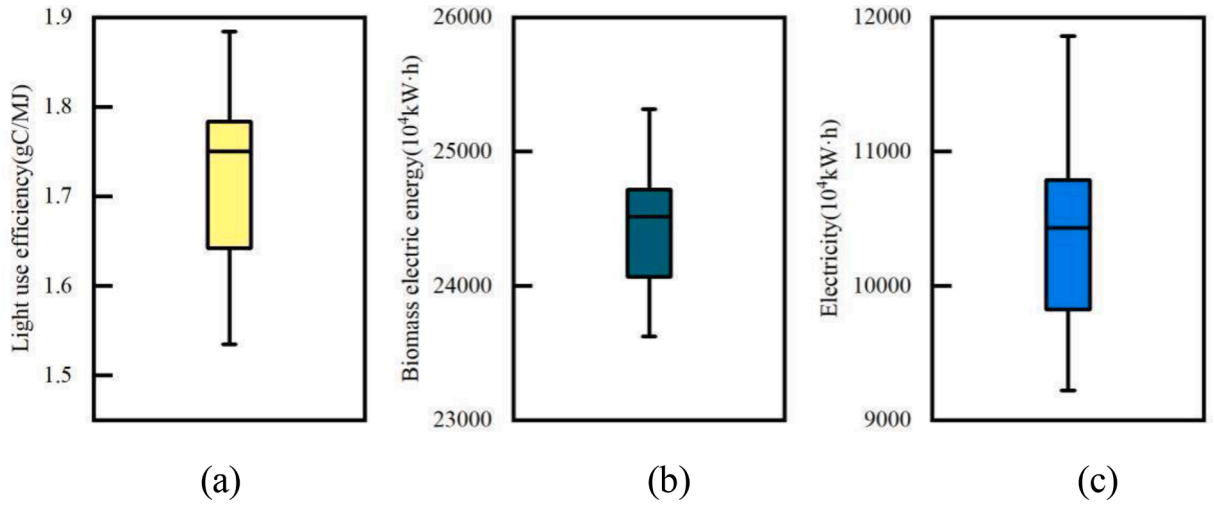

Fig. 8. Energy regulation values.

0.73%], [26.89% ± 0.74%], and [14.30% ± 1.05%], respectively. The distribution ratios of surface water, groundwater and precipitation from May to September were 0.09:0.08:0.83, 0.17:0.14:0.69, 0.15:0.12:0.72, 0.20:0.15:0.65, and 0.11:0.09:0.80, respectively. The surface water and groundwater allocation ratios in May, June, July, and September basically remained the same, and the allocation ratio of surface water to groundwater was slightly higher in August. The low water consumption observed in June, July and August, especially in July, indicates that soybean water shortage issues are most likely to occur in these months, and additional water should be allocated in July as a priority.

5.2. *Planting structure and energy regulation*

Figure 7 shows the planting structures under different scenarios. Under the optimization scenario, the rice, corn, and soybean occupancy ratio was 0.81:0.13:0.06 in the Jinshan subarea, 0.45:0.26:0.29 in the Toulin subarea, 0.95:0.04:0.01 in the Songhuajiang subarea, and 0.77:0.16:0.07 in the Huama subarea. Under the normal scenario, the rice, corn and soybean occupancy ratio was 0.40:0.47:0.13 in the Jinshan subarea, 0.20:0.54:0.26 in the Toulin subarea, 0.70:0.19:0.11 in the Songhuajiang subarea, and 0.40:0.47:0.13 in the Huama subarea. As shown in Fig. 7, rice cultivation is most advantageous, as reflected by the following findings: (1) the crop area allocated to rice crops is much larger than that allocated to corn and soybean crops, and (2) through optimization, the LR-FN-MONLP model considers three mutually balanced objectives (i.e., light use efficiency maximization, biomass electrical energy maximization, and hydroelectric energy minimization) to guarantee the optimal crop area for the different crops within specific adjustable ranges. According to the overall optimal results for the Jinxi Irrigation District, compared to the actual scenario, the percentage of the rice-planted area increased by 61.49%, the percentage of the corn-planted area decreased by 57.77%, and the percentage of the soybean-planted area increased by 4.39%. The LR-FN-MONLP model tended to allocate more area to rice crops, which may occur because the black soil encountered in Heilongjiang can absorb abundant mineral elements, such as nitrogen, phosphorus, and potassium, the quality of rice is good,

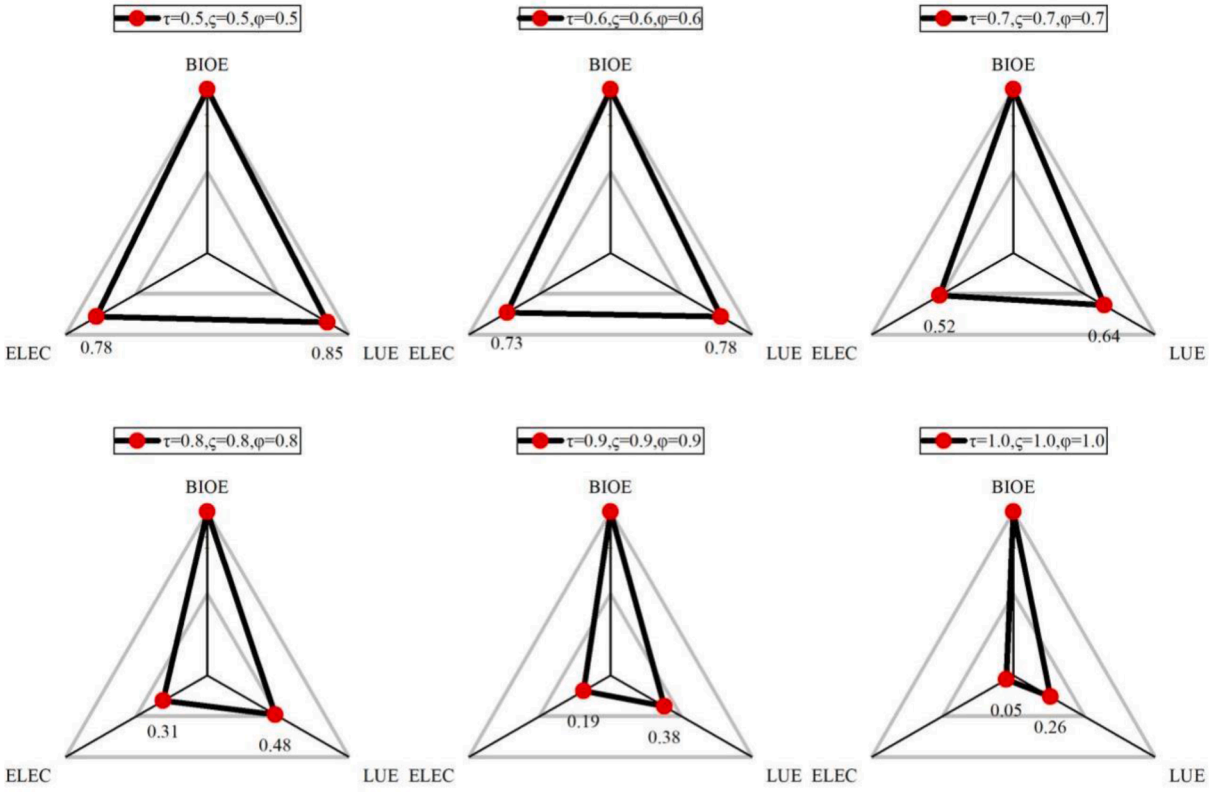

Fig. 9. Trade-off of LUE-ELEC-BIOE under the six confidence level conditions. Note: LUE denotes the light use efficiency; BIOE denotes biomass electricity; ELEC denotes the hydroelectric energy.

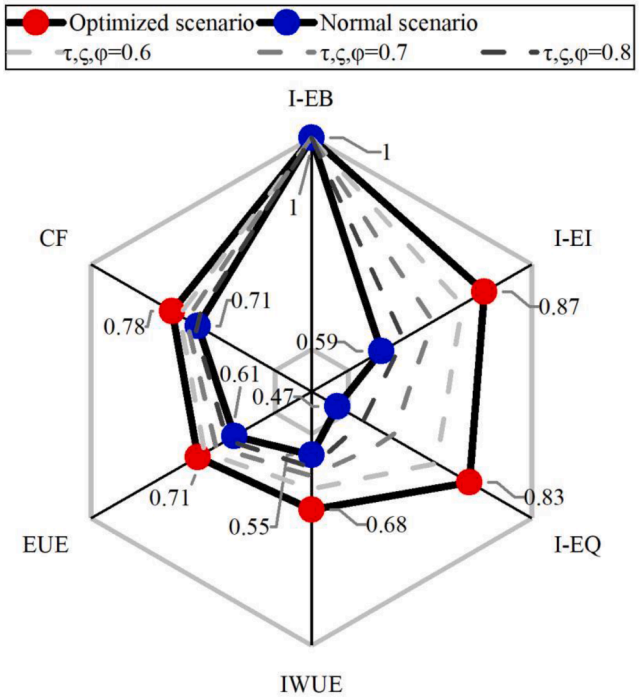

Fig. 10. The trends of multidimensional indicators under different scenarios. Note: I-EB denotes the economic benefits; I-EQ denotes the equity; I-EI denotes the environmental impact; IWUE denotes the irrigation water use efficiency; EUE denotes the energy use efficiency; CF denotes the carbon footprint.

the rice yield per unit area is high, and the water supply in the Jinxi Irrigation District is sufficient. The proportion of rice crops is the largest when $\tau, \varsigma, \phi = 0.5$. As τ, ς, ϕ increases from 0.5 to 1 (where τ, ς, ϕ denotes the variables set by the decision maker to satisfy the probability chance constraint at the lowest confidence level), the proportion of rice crops in different subdivisions gradually decreases, and the proportions of corn crops and soybean crops gradually increase. The results suggest that the lowest confidence scenario yields the most optimal model results, and the sowing of rice crops is emphasized, thus making the allocation of agricultural water, energy, food and land resources more sustainable. However, on the other hand, a lower confidence level means that more water will be allocated, which will increase the water scarcity risk. Moreover, the available electrical energy increases with increasing confidence level in different confidence level scenarios. These findings can guide the future decisions of managers.

The proportion of available electrical energy in the different subareas is as follows: 2555.85×10^4 kW·h (18.46%) in the Jinshan subarea, 6247.91×10^4 kW·h (45.13%) in the Toulin subarea, 973.92×10^4 kW·h (7.03%) in the Songhuajiang subarea, and 4066.27×10^4 kW·h (29.37%) in the Huama subarea. The Toulin subarea exhibits the most available electrical energy, accounting for approximately half of that in the whole irrigation area, followed by the Huama subarea and finally the Jinshan and Songhuajiang subareas. The available power varies little with the confidence level for different confidence levels.

5.3. Multienergy target trade-offs

The optimization model included three objectives related to the light use efficiency, biomass electrical energy, and hydroelectric energy. Additionally, multiple scenarios were generated based on combining the uncertain constraint variables τ, ς, ϕ (all these variables affect agricultural water and soil resource allocation), which impact the objective values. A statistical analysis of the changes in the values of these targets

was performed based on different scenarios, as shown in Fig. 8. In the joint scenario for τ,ς,ϕ, the light use efficiency ranged from 1.53 ~ 1.88 g C/MJ, and the optimized value reached 1.75 g C/MJ. The biomass electrical energy ranged from $2.36 \times 10^8 \sim 2.53 \times 10^8$ kW·h, and the optimized value was 2.45×10^8 kW·h. The hydroelectric energy ranged from $0.92 \times 10^8 \sim 1.19 \times 10^8$ kW·h, and the optimized value reached 1.04×10^8 kW·h. The light use efficiency and hydroelectric energy changed significantly in the different scenarios because both objectives are related to water allocation. Higher confidence levels indicate better satisfaction of the constraints and higher confidence in the optimization results. In particular, a high confidence level corresponds to a low risk of having inadequate surface water and groundwater availability levels. For example, the light use efficiency was the lowest under the conditions of $\tau = 1, \varsigma = 1$ and $\phi = 1$. Fig. 8 shows that the credibility level significantly affects the objectives. This information could guide decision makers in selecting better options in the decision-making process.

Figure 9 shows the model objective function trade-off results under the six confidence level conditions. The different scenarios in the figure represent different credibility level scenarios (τ, ς, ϕ from 0.5 to 1). The area of the triangle represents the degree of coordinated development, and a larger area represents better coordinated development for a given scenario. The vertices of BIOE, LUE, and ELEC represent the optimal values of the three different objectives, and the closer to the vertices an indicator plots, the stronger the indicator is. Specifically, in each scenario, each objective function value remains between the corresponding maximum and minimum values, and by determining the upper and lower possible levels for each objective, the range of each objective can be determined. Then, via the application of normalization methods (details given in the Supplementary Materials), the indicator value of each objective can be determined. As an indicator value increasingly approaches 1, the indicator better satisfies the needs of the decision maker. For example, for $\tau = 0.6, \varsigma = 0.7$, and $\phi = 0.8$, if only the light use efficiency target is considered, the light use efficiency will reach 2.03 g C/MJ. If only the biomass electrical energy usage target is considered, the biomass electrical energy will reach 2.75×10^8 kW·h. If only the hydroelectric energy target is considered, hydroelectric energy will reach 0.78×10^8 kW·h. However, considering these three objectives simultaneously, the light use efficiency will reach 1.75 g C/MJ, the biomass electrical energy usage will be 2.45×10^8 kW·h, and the hydroelectric energy will total 1.04×10^8 kW·h. These results reveal that a trade-off occurs among these three objectives, and a rational allocation result is obtained from a synergistic multienergy perspective. However, numerically, the biomass electrical energy indicator was notably stable in the different scenarios, with values close to 1, and the light use efficiency and hydroelectric energy targets varied considerably. The degree of coordination in the model [31] decreased with increasing confidence level, with values of 0.93, 0.91, 0.83, 0.73, 0.65, and 0.48. The results indicate that the model solutions with lower confidence levels yield higher satisfaction than do those with higher confidence levels (as shown in the figure below; notably, the model results with lower confidence levels encompass a larger area than that based on the model results with higher confidence levels), which facilitates the sustainable allocation of agricultural water, energy, food and land resources. However, a lower confidence level is associated with a higher risk of water scarcity due to the allocation of additional water resources, and this relationship can guide the future decisions of decision makers. These results suggest that a balanced decision approach could be established if the light use efficiency, hydroelectric energy and biomass electrical energy usage are simultaneously considered.

5.4. Model multidimensional effect evaluation

Figure 10 shows the six individual objectives related to economic, environmental and social factors, the irrigation water use efficiency, the energy use efficiency, and the carbon footprint under different scenarios. Notably, the model optimization results were analyzed through a comparison to the current conditions. First, the value of each objective function plots within the range of the maximum and minimum values. By determining the upper and lower achievable limits of each objective, the range of each objective can be determined, and the indicator value of each objective can then be determined through normalization. As an indicator value tends to approach 1, the satisfaction level of decision makers is enhanced. The figure shows that the total area in the optimal scenario is larger than the total area in the actual scenario, i.e., the optimal scenario increases the satisfaction level of decision makers compared to that for the actual scenario (a coordinated development degree of 0.90 under the optimal scenario and a coordinated development degree of 0.79 under the actual scenario; for $\tau, \varsigma, \phi = 0.6, \tau, \varsigma, \phi = 0.7$, and $\tau, \varsigma, \phi = 0.8$, the values are 0.87, 0.85 and 0.82). The indicators of the economic dimension are robust and close to 1 in each scenario, and the indicators of the environmental and social dimensions change more significantly. The irrigation water use efficiency, energy use efficiency, and carbon footprint are generally less variable. The coordinated development of the model decreases with increasing confidence value (i.e., as the value of τ, ς, ϕ decreases from 0.6 to 0.8) (shown in the figure as the area of the enclosed hexagon, which decreases with increasing confidence value). The results show that the models with lower confidence levels yield better satisfaction results than the models with higher confidence levels (as reflected by the larger area of the graphs obtained for models with lower confidence levels); however, such results are also associated with a higher risk of water shortage. Due to the reduction in the total land allocation amount in the optimized case, both the benefits and costs decrease, resulting in 9.58% lower net system benefits than those under the actual scenario. However, pollutant emissions are reduced by 22.01%, resource allocation equity is improved by 7.85%, the water use structure is impacted by adjusting the cropping structure, and the irrigation water use efficiency is improved by 2.67%. Moreover, the energy use efficiency increases by 4.92%, and the carbon footprint decreased by 5.38%. The model developed in this paper could help decision makers manage agricultural water and soil resources in a more sustainable way.

6. Conclusion

This study provides an optimization pathway for the sustainable development of WEFN systems in irrigated agricultural areas. A modeling approach for the synergistic and optimal regulation of water and soil energy resources in WEFN systems is established from a coordinated multienergy perspective. The characteristics and advantages of the developed approach can be summarized as follows: (1) The proposed approach can help achieve trade-offs among the light use efficiency, biomass electrical energy utilization, and hydroelectric energy use. (2) The model can help decision makers understand the overall scheme of water allocation in irrigation areas and assess the ratio of water consumption to water demand (relative water consumption) in each growth stage throughout the water cycle, thus effectively considering water scarcity and the associated influence on the yield in each growth stage. (3) The allocation of limited agricultural water and land resources is optimized to provide a reference for sustainable agricultural development. (4) The adoption of LR-type fuzzy numbers and uncertainty methods with possibilistic mean value and credibility constraints not only helps reflect the uncertainty in model parameters (e.g., the maximum light use efficiency, pump efficiency, and crop yield per unit area) but also aids in generating model solutions through different objective functions; therefore, this approach can enable decision makers to objectively address the actual problems in agricultural water and land resource allocation.

The application value of the model constructed in this paper for the synergistic optimization of water-land-energy resources in WEFN systems from the perspective of multienergy synergy in irrigation districts is mainly reflected in the ability of the model to promote the efficient management of agricultural water, land, and energy resources and to

enhance the ability of irrigation districts to cope with changes in energy sources. The results of the model can provide practical guidance for the management of agricultural water, land and energy resources in the Jinxi Irrigation District. For example, (1) surface water is the main water supply source, and the optimal ratio of surface water to groundwater is 7:2. June and July are critical periods for irrigation and are the most sensitive to water shortages, so the ratio should be adjusted in June and July given the limited water resources. (2) A balance is achieved among biomass electrical energy, hydroelectric energy, and light use efficiency. A 8.57% increase in the light use efficiency leads to a 6.65% decrease in hydroelectric energy and a 1.39% increase in biomass energy. The optimal allocated volume of surface water is 2.11×10^8 m^3, and that of groundwater is $0.592.11 \times 10^8$ m^3. Based on these allocations, the planting ratio of rice, corn and soybean crops is 5.02:1.43:1.21. Fluctuations in the water supply have a significant impact on the utilization rates of light energy and hydroelectric energy; notably, when the quantity of available water increases by 4.16%, the light use efficiency will increase by 6.28%, and the hydroelectric energy will decrease by 4.17%. In this case, the planted area could be increased by 3.09%, however, no further adjustments on plantation structure are required. According to the model results, decision makers can realize the optimal water and soil distribution patterns and synergistic multienergy utilization. Additionally, water resource trends can be predicted in advance to appropriately adjust energy and agricultural resource utilization schemes. (3) Due to the reduction in land area under the optimal scenario, the net benefit of the system is reduced by 9.58%. However, pollutant emissions are reduced by 22.01%, the resource allocation equity is improved by 7.85%, the water use structure is enhanced by adjusting the planting structure, the irrigation water use efficiency is improved by 2.67%, the energy use efficiency is increased by 4.92%, and the carbon footprint is reduced by 5.38%. Thus, the developed model can allow decision makers to manage agricultural soil and water resources in a more sustainable manner.

The developed model can be applied to other regions or water and soil resource allocation problems to provide decision makers with suitable strategies. In this paper, we consider the WEF relationship from the synergistic perspectives of light use efficiency, biomass electrical energy, and hydroelectric energy. However, there is limitation to consider the relationship between recycling and transformation of the three energy sources in irrigated agriculture, and the mathematical approach to coupling the three energy objectives into a single objective can consider other approaches (e.g. multi-objective algorithms to find Pareto solutions, etc.).

CRediT authorship contribution statement

Mo Li: Formal analysis, Funding acquisition, Methodology, Writing – review & editing. **Li Zhao:** Methodology, Software, Writing – original draft. **Chenglong Zhang:** Formal analysis, Investigation. **Yangdachuan Liu:** Data curation. **Qiang Fu:** Supervision.

Declaration of Competing Interest

The authors declare that they have no known competing financial interests or personal relationships that could have appeared to influence the work reported in this paper.

Acknowledgments

This research was supported by the National Natural Science Foundation of China (52079029), and the Key Laboratory Program of Ministry of Agriculture and Rural Affairs of the People's Republic of China (AWR2021001).

Appendix A. Supplementary data

Supplementary data to this article can be found online at https://doi.org/10.1016/j.enconman.2022.115537.

References

[1] Karabulut AA, Crenna E, Sala S, Udias A. A proposal for integration of the ecosystem-water-food-land-energy (EWFLE) nexus concept into life cycle assessment: a synthesis matrix system for food security. J Cleaner Prod 2018;172:3874–89.
[2] Shu Q, Scott M, Todman L, McGrane SJ. Development of a prototype composite index for resilience and security of water-energy-food (WEF) systems in industrialised nations. Environ Sustain Ind 2021;11:100124.
[3] Okonkwo EC, Abdullatif YM, Al-Ansari T. A nanomaterial integrated technology approach to enhance the energy-water-food nexus. Renew Sustain Energy Rev 2021;145:111118.
[4] FAO. "Energy-smart" Food for People and Climate. Food and Agriculture Organization of the United Nations (FAO), (2011).
[5] Endo A, Tsurita I, Burnett K, Orencio PM. A review of the current state of research on the water, energy, and food nexus. J Hydrol: Reg Stud 2017;11:20–30.
[6] Ren CF, Xie ZS, Zhang Y, Wei X, Wang YS, Sun DY. An improved interval multi-objective programming model for irrigation water allocation by considering energy consumption under multiple uncertainties. J Hydrol 2021;602:126699.
[7] Ma Y, Li YP, Zhang YF, Huang GH. Mathematical modeling for planning water-food-ecology-energy nexus system under uncertainty: a case study of the Aral Sea Basin. J Cleaner Prod 2021;308:127368. https://doi.org/10.1016/j.jclepro.2021.127368.
[8] Zuo Q, Wu Q, Yu L, Li Y, Fan Y. Optimization of uncertain agricultural management considering the framework of water, energy and food. Agric Water Manag 2021;253:106907.
[9] Zhang X, Vesselinov VV. Integrated modeling approach for optimal management of water, energy and food security nexus. Adv Water Resour 2017;101:1–10.
[10] Davijani MH, Banihabib ME, Anvar AN, Hashemi SR. Multi-objective optimization model for the allocation of water resources in arid regions based on the maximization of socioeconomic efficiency. Water Resour Manage 2016;30:927–46.
[11] Catolico ACC, Maestrini M, Strauch JCM, Giusti F, Hunt J. Socioeconomic impacts of large hydroelectric power plants in Brazil: a synthetic control assessment of Estreito hydropower plant. Renew Sustain Energy Rev 2021;151:111508. https://doi.org/10.1016/j.rser.2021.111508.
[12] Borges AdV, Fuess LT, Alves I, Takeda PY, Damianovic MHRZ. Co-digesting sugarcane vinasse and distilled glycerol to enhance bioenergy generation in biofuel-producing plants. Energy Convers Manage 2021;250:114897.
[13] Gonçalves AL, Simões M, Pires JCM. The effect of light supply on microalgal growth, CO2 uptake and nutrient removal from wastewater. Energy Convers Manage 2014;85:530–6.
[14] Jiang S, Huang Y, Zhao L, Cui N, Wang Y, Hu X, et al. Effects of clouds and aerosols on ecosystem exchange, water and light use efficiency in a humid region orchard. Sci Total Environ 2022;811:152377.
[15] Wiranarongkorn K, Phajam P, Im-orb K, Saebea D, Arpornwichanop A. Assessment and analysis of multi-biomass fuels for sustainable electricity generation. Renewable Energy 2021;180:1405–18.
[16] Green WH, Ampt GA. Studies on soil physics I. The flow of air and water through soils. Int J Nonlinear Sci Numerical Simul 2015;4:1–24.
[17] Pérez-Cañedo B, Concepción-Morales ER. On LR-type fully intuitionistic fuzzy linear programming with inequality constraints: Solutions with unique optimal values. Expert Syst Appl 2019;128:246–55.
[18] Zhang Q, Li Z. Data-driven interval credibility constrained quadratic programming model for water quality management under uncertainty. J Environ Manage 2021;293:112791.
[19] Mavrotas G. Effective implementation of the ε-constraint method in Multi-Objective Mathematical Programming problems. Appl Math Comput 2009;213:455–65.
[20] Carlsson C, Fullér R. On possibilistic mean value and variance of fuzzy numbers. Fuzzy Sets Syst 2001;122:315–26.
[21] Liu B, Liu YK. Expected value of fuzzy variable and fuzzy expected value models. IEEE Trans Fuzzy Syst 2002;10:445–50.
[22] Li L, Yao Z, You S, Wang CH, Chong C, Wang X. Optimal design of negative emission hybrid renewable energy systems with biochar production. Appl Energy 2019;243:233–49.
[23] Li M, Fu Q, Singh VP, Liu D, Li J. Optimization of sustainable bioenergy production considering energy-food-water-land nexus and livestock manure under uncertainty. Agric Syst 2020;184:102900.
[24] Potter CS, Randerson JT, Field CB, Matson PA, Vitousek PM, Mooney HA, et al. Terrestrial Ecosystem production: a process model based on global satellite and surface data. Global Biogeochem Cycles 1993;7(4):811–41.
[25] Vito RD, Portoghese I, Pagano A, Fratino U, Vurro M. An index-based approach for the sustainability assessment of irrigation practice based on the water-energy-food nexus framework. Adv Water Resour 2017;110:423–36.

[26] Scott JG, Stephen DP, Samuel N, Goward MM, Thawley JS. Satellite remote sensing of primary production: an improved production efficiency modeling approach. Ecol Model 1999;122(3):239–55.
[27] Cui Y, Liu J, Hu Y, Bing L, Tao F, Wang J. Estimation and analysis of the optimum temperature for vegetation growth in China. J Nat Resour 2012;27:12.
[28] Chen X, Cui Z, Fan M, Vitousek P, Ming Z, Ma W, et al. Producing more grain with lower environmental costs. Nature 2014;514:486–9.
[29] Li J, Shang S, Jiang H, Song J, Rahman KU, Adeloye AJ. Simulation-based optimization for spatiotemporal allocation of irrigation water in arid region. Agric Water Manag 2021;254:106952.
[30] Wang Y, Bi Y, Gao C. Evaluation of the amount of straw resources that can be collected and utilized in China and its suitability. China Agric Sci 2010;43:1852–9.
[31] Yang WC, Xu K, Lian JJ, Bin LL, Ma C. Multiple flood vulnerability assessment approach based on fuzzy comprehensive evaluation method and coordinated development degree model. J Environ Manage 2018;213:440–50.